OPTIMISING THE MORPHOLOGY OF ADDITIVELY MANUFACTURED EARTHEN FACADE ELEMENTS

Leslie Ing
Faculty of Architecture & the Built Environment, Delft University of Technology
Julianalaan 134, 2628BL Delft

ABSTRACT

This paper examines the relationship between the material properties of AME mixtures and optimal design solutions of a cavity wall facade based on structural, thermal and efficiency objectives. This is done through a process of inventorying the influence of additive manufacturing on the properties of earth mixtures, establishing the numeric requirements for a functional earthen facade and defining the inputs to generate valid thermal and constructive evaluation results. Through a parametric model, facade elements are generated that are optimised on multiple objectives. It is demonstrated that earth has a lot of potential when combined with AM, potentially resulting in a more efficient and sustainable way of construction. However, further research is needed before application in real-world scenarios becomes feasible.

KEYWORDS: *Additive manufacturing, Earthen facade, Multi-objective optimisation, Wind load, Insulation*

I. INTRODUCTION

In the 80s it was estimated that around 33 percent of the global population inhabited an earthen dwelling, but today that number has decreased to 8-10 percent (Marsh & Kulshreshtha, 2022). Building with earth is increasingly seen as something from the past because a house is considered 'modern' and attractive when built with materials such as concrete, steel and bricks (Hall et al., 2012). Such 'non-traditional' materials however are high in embodied energy and have a large carbon footprint when compared to earth (Cabeza et al., 2013). Furthermore the raw resources used in their production don't renew at the rate they are consumed. Because we are globally aiming to reduce our carbon footprint, we will have to reduce our dependence on these scarce building materials by exploring alternative materials and construction methods.

At the same time there is an enormous demand for new housing as a consequence of growing populations and urbanisation, especially in developing countries. These two factors together will add an estimated 2.5 billion to the world's urban population by 2050, of which almost 90 % will be born in Asia and Africa (United Nations, 2019). All these people will need to be supplied with affordable, adequate, and safe housing. This global housing demand is not exclusive to the developing world, as even in an already heavily urbanised and dense country such as the Netherlands a million houses are planned to be built by 2030 (Groenemeijer, 2021). Developed countries should take the lead in promoting the use of sustainable and abundantly available building materials such as earth. Both because of the debt owed to the developing world thanks to the historical overconsumption of resources and energy, but also because of the soft power 'western' architecture has on what is considered 'modern' housing.

Although there exists a rich and global tradition of earthen dwellings, the material needs to undergo a revolution to make it popular again. A paradigm shift towards the use of such an ancient building material in modern construction might be accomplished twofold. On one hand the material needs to be evaluated on technical terms, by (re)understanding its technical properties so as to investigate its potential in modern construction. On the other hand, the material will have to be presented as architecturally desirable in order to be associated with sustainability and improved living standards, instead of the past and poverty. A promising place where these technical and architectural considerations intersect is in the act of 3D printing, or additive manufacturing (AM).

The potential benefits of combining earth and AM (AME) in modern construction are being heavily studied in academics (Endres et al., 2021). Over the course of history different building techniques using earth were developed in accordance with the local climatic conditions, using whatever could be locally sourced. AME is the most recent of such phenomena, thanks to developments in the 3D printing sector and material science. Different from rammed earth (RE) or compressed earth bricks (CEB), additive manufacturing requires a more viscous earthen mixture which is extruded like a paste, layer by layer and following the machine's toolpath. This allows for a high degree of form and design freedom when compared to formworks, as it enables mass customisation of the created elements.

One of the most critical elements of a habitable building is its facade. By combining high-tech AM fabrication methods with low-tech material such as earth, new architectural morphologies of the earthen facade are to be developed. These morphologies can contribute towards a sustainable built environment when energy, material and structural efficiency are in balance. The goal of this paper is to explore that potential in the Dutch context through a multi-objective optimisation process, in which the technical properties of additively manufactured earth are expected to be reflected in the generated facade morphology. Thus the overall research question of the paper is the following:

"How is the optimisation of an additive manufactured earthen facade for insulating capability and structural integrity reflected in its architectural morphology?"

To answer this question the following necessary sub-questions are formulated:

"How does additive manufacturing influence the properties of earth mixtures?"

"What are the numeric requirements for a functional earthen facade?"

"What are the necessary inputs to produce valid thermal and constructive evaluation results?"

II. Method

In the sub-sections of section III, *Literature review and definitions*, the prerequisite qualitative and quantitative information for the optimisation process will be collected and the sub-questions answered. This state of the art literature research will support the technical validity of the results of the optimisation. In section IV, *Optimisation and evaluation of insulated AME cavity wall facades*, a proposed sinusoidal facade element will be optimised and evaluated based on multiple objectives.

Because of limitations in the large-scale scale testing of physical prototypes, this paper will approach the optimisation and evaluation part of the research computationally. This is achieved through a process of research by design, centred in the episteme of morphology, or the study of the evolution of form in the built environment. To do so, Rhinoceros 3D (6) and the visual programming interface Grasshopper are used. With the Honeybee Legacy plug-in for Grasshopper, THERM (7.6) is accessed for 2D heat transfer evaluations of horizontal sections of the designs. The plug-in Karamba3D is used for structural analysis, using the finite element method analysis (FEA).

When the amount of variations of facade elements becomes too large for human evaluation as a result of the amount of variables, a process of algorithmic optimisation can be employed which is known as generative design. This is done in Grasshopper using the Wallacei plug-in's evolutionary algorithms. By inputting the variable parameters (genotypes), the evolutionary solver will be able explore the design space by optimising the morphology (phenotype). This is based on criteria (fitness objectives) which, like the parameters, are quantitative values defined by the computational designer. The results of the optimisations will be visualised through numeric performance and figures showing the optimised additive manufactured earthen facade morphologies.

Then, in section VI, *Conclusion*, the main research question of how the optimisation of an additive manufactured earthen facade for insulating capability is reflected in its architectural morphology is answered. The final section VII, *Discussion*, is used to bring attention to limitations in the research as well as future research opportunities.

III. Literature review and definitions

3.1. The influence of additive manufacturing on the properties of earth mixtures

3D printed samples of earthen mixtures and their structural and load-bearing properties were investigated by Perrot et al. (2018), Gomaa et al. (2021) and Ferretti et al. (2022a). The base of such mixtures, colloquially known as earth or soil, consist of sand, silt and clay particles of different sizes. One way to categorise these compositions is by soil texture, which depends on the ratio in which these components are combined. A mixture of 40% sand, 40% silt and 20% clay, for example, is considered a loam. The (structural) properties of the material can be improved through additives, which is a condition for printing functional earthen elements.

Perrot et al. (2018) used a seaweed biopolymer as a binder in the earth mixture and mechanically tested its impact on structural performance. The research showed that the alginate improved the speed at which the Young's modulus developed with a minimal impact on the final compressive strength, which remained in the same order of conventional cob earth, potentially enabling the printing of an earthen wall of 3 metres tall within a single day. Gomaa et al. (2021) used an earth mixture likened to cob because of the addition of straw fibres. They showed that this 3D printed cob exhibits similar compressive characteristics as conventional cob through experimental tests and would be able to act as load-bearing in two-storey buildings. Furthermore they used the resulting data to computationally optimise different wall-cross section patterns which showed that it is possible to create structurally more efficient hollow wall sections compared to conventional solid wall sections.

Ferreti et al. (2022b) tested biocomposites to stabilise earthen mixtures, consisting of (un)shredded rice husk and lime. Rammed cubic specimens were subjected to uniaxial compression tests. In these earth mixtures the hardening in the long term resulted in vulcanisation, which occurred thanks to mineralisation of the vegetable fibre by carbonation of the lime. Ferretti et al. expanded the research to test the load-bearing capacities of the mixture with shredded rice husk in 3D printed specimens (2022a). The compressive strength under mechanical testing of the elements saw results similar to that of the elements from the previous paper (2.50 MPa), around 2.32 MPa, evidencing that the layer by layer extrusion process had little to no impact on the strength of the earth mixture. Furthermore it was discovered that the infill of the hollow wall element had a structural function by stopping cracks.

Through tests of the tensile strength of earth layers and between layers by Bui et al. (2014) it was concluded that rammed earth can be considered an isotropic material in tension. We will consider our layer by layer additively manufactured earth to behave similarly. One of the major benefits of using earth is its abundance and harvesting close to the construction site, which suggests the need to develop a new mixture depending on the local soil conditions and available resources. However, for the research in this paper, a mixture with shredded rice husks and lime used by Ferretti et al. in 2022 are used (See Table 1), since its properties have been well documented with a proven history in small scale building projects. Its main component is a calcareous loam with a dry density of 1815 kg/m^3. An unspecified amount of mixing water is added for extrudability depending on the climatic conditions.

Table 1. Percentage composition by weight of the earth mixture (Adapted from Ferretti et al., 2022a, b).

Component	**Mixture**
Soil (30% clay, 40% silt and 30% sand)	70.42%
Lime-based binder	4.70%
Hydraulic lime	4.69%
Shredded rice husk	1.41%
Silica sand	18.78%

The assumed structural and thermal properties of the mixture are seen in Table 2. The compressive strength of 2.32 MPa is based on tests done by Ferretti et al. (2022a), but no information is available on tensile strength. For rammed earth it is often given a value of 10% of the compressive strength (Ávila et al., 2021). In a study by Araki et al. (2016) comparing rammed earth mixtures without and with lime, the tensile strength improved from 5.0-12.5% to 15-20% of the compressive strength after 28 days through the addition of lime. Since our mixture uses a reasonably similar amount of lime (9.39%) to the one tested (8.20%), we went with an improved but lower boundary of 15% to calculate the tensile strength.

Feretti et al. (2022a) found a Poisson's ratio (v) of 0.214 at maximum stress, comparable to Perrot et al. (2018) who found a mean value of 0.22. From the latter research the Young's modulus' (E) mean value of 22.9 MPa was used. Perrot et al.'s mixture was established as having a 23% moisture content after printing, but no data was made available on the potential influence of drying on its development over time. Based on the defined values the in-plane and transverse shear moduli (G) are calculated:

$$G = \frac{E}{2 \cdot (1+v)} = \frac{22.9}{2 \cdot (1+0.214)} = \frac{22.9}{2.428} = 9.43\ MPa$$

The earth mixture's thermal expansion coefficient, like in the shotearth research by Feng (2021), was defined as a negligible 0.00001 or the coefficient of concrete. Furthermore the value of 20.3 kN/m^3 was used for the specific weight of our mixture: the general specific weight of soil.

To understand the thermal properties of the mixture we assumed it to be a silt and clay soil, because even with the additional sand the percentage of silt and clay in the used soil is relatively high. The effects of the additives on the thermal properties are ignored because of their small part in the mixture. With a dry density of close to 1800 kg/m^3, the thermal conductivity of the material at 20% water saturation is defined as 0.65 W/(m·K) (Farouki, 1988). This appears to be in the same order of magnitude as 3D printed cob samples tested by Gomaa et al. (2019). According to measurements by Rubio et al. (1997) clayey soils have an emissivity value of 0.957 ± 0.005. We will round this value down to 0.95. Lastly, a lack of data on solar absorptivity makes us use a default value of 0.5.

Table 2. Assumed structural and thermal properties of the earth mixture.

Property	**Value**	**Unit**
Young's modulus (E)	22.9	MPa
Poisson's ratio (v)	0.214	Between 0-0.5
In-plane shear modulus (G)	9.43	MPa
Transverse shear modulus (G)	9.43	MPa
Specific weight (γ)	20.3	kN/m^3
Thermal expansion coefficient	0.00001	1/℃
Compressive strength	2.32	MPa
Tensile strength	0.348	MPa
Conductivity (λ)	0.65	W/(m·K)
Solar absorptivity	0.5	Between 0-1
Emissivity	0.95	Between 0-1

3.2. Numeric requirement for a functional earthen facade

The earthen facade in our research is defined as a non-load bearing element, distinct from an interior wall for its characteristic of protecting the interior of a building from the outdoor conditions and retaining comfortable indoor conditions. We are interested in how the facade withstands the wind but also how the temperature in the building can remain comfortable. For the sake of limiting the scope of our research, our facade morphology is further defined as an element without openings, 3 metres wide and with variable thickness and infill. Finally it's extruded vertically to a height of 3 metres.

The performance of a facade can be quantified into measurable fitness objectives. In the computational model they are reduced to the ones displayed in Table 3. We will optimise for area (m^2), total width of construction (mm), R-value ($W/(m^2 \cdot K)$), utilisation (%) and displacement (cm). The area and width of construction should be limited in order to preserve material and improve usable space inside and are thus to be minimised in the optimisation process. Since the structural and insulative capability of the facade are more specific, they are not simply to be maximised or minimised but rather should converge to the required standard while discarding those design options that don't comply with the objective requirements through an added penalty. In the case of the Netherlands the minimum R-value for new built constructions is 4.5 $W/(m^2 \cdot K)$. In order to prevent material failure the utilisation should be as close to 100% as possible without exceeding it. A maximum displacement (s) of a facade is not established in any Dutch norm, so instead we will use the NEN-EN 1990 norm for the maximum displacement of a roof using the formula as adapted from Arends et al. (2022):

$s \leq 0.004 \cdot height \qquad s \leq 0.004 \cdot 300\ cm \qquad s \leq 1.2\ cm$

Table 3. Defined objectives for a functional earthen facade.

Property	**Fitness objective**	**Unit**
Used area of material	Minimise	m^2
Total width of construction	Minimise	mm
R-value	≥ 4.5	$W/(m^2 \cdot K)$
Utilisation	≤ 100	%
Max. displacement (s)	≤ 1.2	cm

3.3. Inputs for valid thermal and constructive evaluation results

In order to evaluate the facade elements, Grasshopper inputs are defined, see Appendix Figure 1. For the THERM exterior and interior conditions, temperatures of -10 ℃ and 20 ℃, respectively, were used based on the Dutch climate conditions (ΔT = 30). Two different types of loads are identified as Karamba3D inputs. First there is the gravity load in which gravity is assumed to be 10 m/s^2. Secondly there are the horizontal wind loads acting locally on the face of the facade element which are determined using NEN-EN 1991-1-4 (Arends et al., 2022). They encompass the positive external pressure (F_e) and the negative internal pressure (F_i) acting on the exterior and interior respectively. It is determined that the force coefficients (c_f) for those are 0.8 and -0.3. For the calculation we make the assumption that the top edge of our facade is found on a height of 9 m (third storey) in the most windy zone of the Netherlands (coastal region 1) and is sheltered by buildings. This results in an 'extreme thrust pressure' ($q_p(z_e)$) of 0.77 kN/m^2. The simplified calculations for the wind loads then are:

$F_e = c_f \cdot q_p(z_e) = 0.8 \cdot 0.77 = 0.616\ kN/m^2$

$F_i = c_f \cdot q_p(z_e) = -0.3 \cdot 0.77 = -0.231\ kN/m^2$

IV. Optimisation and evaluation of insulated AME cavity wall facades

The thermal properties of earth alone are not suitable for moderate climates, since a high thermal mass is not enough to retain a comfortable indoor climate without using a large amount of energy. However a very thick and solid earthen wall, notwithstanding the mentioned disadvantage, can still keep the cold outside and heat inside. The required thickness (d) can be simply calculated by multiplying the desired R-value of 4.5 W/($m^2 \cdot K$) with our determined thermal conductivity (λ) of 0.65 W/(m · K):

$$d = R \cdot \lambda = 4.5 \cdot 0.65 = 2.95\, m$$

A facade of 2.95 m thick is extremely inefficient as far as material usage and usable floor area is concerned. Adding an insulating material should be key to reduce the earthen facade's size. This can be accomplished by splitting the facade in two and creating an earth cavity wall filled with insulation.

Sheep wool is a biobased material with the ability to perform well under moist conditions and could be used to fill the cavities in 3D printed damp open earth mixtures. This material will be used in the evaluation of the parametric model and has a similar thermal conductivity (0.038-0.054) to widely used insulation materials like EPS, XPS and Rock Wool that range between values such as 0.031-0.043 (Asdrubali et al., 2015). At the same time it has substantially less of an embodied energy footprint and global warming potential. An average conductivity of 0.046 W/(m · K), solar absorptivity and emissivity values as the default values of 0.5 and 0.9 respectively, are assumed.

One of the major areas of interest with 3D printing is creating unique and complicated geometries, compared to traditional methods of construction. This fact is exploited in the creation of the parametric model for an insulated AME cavity wall, through using the concept of the sinusoidal wall. By creating the external wall in a wave pattern it is hypothesised that it uses less material for the same stability as a straight wall. The trade-off would be the bigger footprint of the wall by reducing the potential functional space of the building. Such a sinusoidal facade is made possible through 3D printing, where no complicated formwork and ramming methods are required. The interior wall is kept straight to compare to the effects of the sinusoidal wall. Both walls are kept separate and will deal with their own wind load in either pressure or suction.

5.1. Method

For the Grasshopper script see Appendix Figure 1. Five variable parameters or genotypes are used to describe the morphologies of the cross-sections. By varying these parameters; the amplitude, amount of waves and thickness of the sinusoidal external wall, the depth of the cavity with its insulation and the depth of the interior wall, different facade elements can be created. These variables are directly related to two out of seven objectives: the minimisation of the total area used by the facade including the insulation and the minimisation of its width.

For the 2D thermal evaluation with THERM the thermal properties used are the sheep wool insulation as previously mentioned and the earth mixture from Table 2. The boundary conditions as mentioned in sub-section 3.3 are used. The objective here is to have a R-value close to 4.5 W/(m2 · K). This is done by minimising the difference between the actual value and the desired value. In order to discard invalid facade elements there is a penalty applied to the elements that are lower than the desired value.

The cross-sections of the two wall elements are extruded as described in sub-section 3.2 for structural evaluation with Karamba3D, see Appendix Figure 2. The insulation is discarded as having no structural properties and not taken into account. The two walls are supported at the bottom and top and together form the facade. The structural properties of earth as described in Table 2 are used for the wall material properties. Both walls are evaluated separately on both displacement and utilisation, resulting in four more objectives. The displacement score is calculated by minimising the displacement, with a penalty when it is larger than 1.2 cm. For the utilisation the absolute values are taken and the largest out of these values is maximised, with a penalty when larger than 100 %.

Finally the evolutionary solver Wallacei is configured for 20 generations of 50 individuals, see Appendix Figure 3. Within this design space the optimal design solutions will be searched for through the multi-objective optimisation process which automatically alters the Genotypes and calculates the fitness scores of each objective. As output or Phenotype THERM meshes are generated.

5.2. Results

After starting the Wallacei optimisation it took around 40 minutes to generate 1000 design options, as can be confirmed in the RunTime information in Appendix Figure 4. The following graphs and figures are generated by Wallacei.

Figure 1. Standard Deviation Graph, Parallel Coordinate Plot and Objective Space.

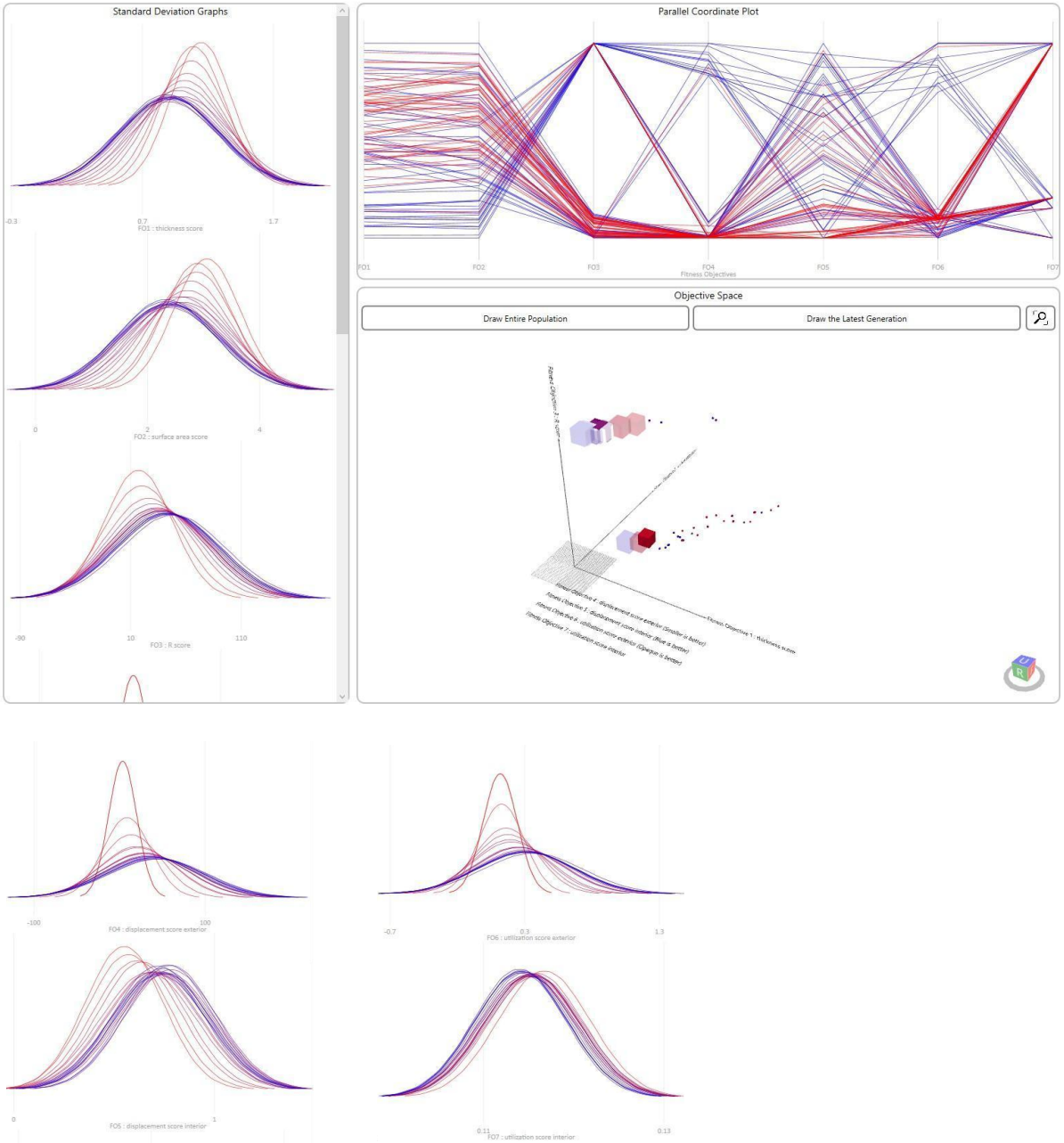

5.3. Evaluation

There are some observations to make from the results in Figure 1. In the Standard Deviation Graph every generation is represented by a graph from earlier generations in red towards recent generations in blue. The scores for thickness (FO1) and surface area (FO2) over time are trending to the left, or towards an improved score, but at the same time the values become more diverse.

For the R-value score (FO3) the generations skew to the right over time, meaning the solutions are receiving a score which is less close to the desired value. This might be influenced by the built in penalty which negatively impacts the score, or because the area and thickness scores weighted heavier and led towards more favourable design options that are thinner and smaller but have worse scores in the thermal performance.

The same appears to be the case for the displacement (FO4) and utilisation (FO6) scores of the exterior wall. However in the interior wall evaluation there is a remarkable difference between the displacement score (FO5) and the utilisation score (FO7), as the displacement score standard deviation graphs is similar to that of the exterior walls, but the utilisation trends towards the left within a similar width of scores. This might be explained by the simple geometry which would tend to become as thin/small as possible while still achieving acceptable utilisation results in comparison to the more convoluted sinusoid wall where the amplitude and amount of waves have a stronger reciprocity with the scores.

Furthermore, when observing the Parallel Coordinate Plot it can be seen that FO1 and FO2 are almost linearly related, since the thickness of the facade and the area impact each other directly. However the sinusoid wall variables such as the amplitude may reduce the area only a little in exchange for a bigger thickness. Another observation are the peaks in the other Fitness Objectives. This is the result of the applied penalties which worsen the scores by a lot in order to differentiate them as unusable.

Those peaks can be observed in the Objective Space, where all the design solutions are plotted in three axes: FO1, FO2 and FO3. Better scores are supposed to trend to the 0,0,0 point in the Objective Space. It can be seen that since the R-value is given a penalty when lower than the desired value, two distinct sets of solutions are visible.

In order to better understand the resulting morphologies of the multi-objective optimisation we use the K-means clustering algorithm which is part of the Wallacei package. See Appendix Figure 5 for the clustering settings. By clustering the pareto front of the last generation or most optimal solutions, the solutions which objectively outperform all other solutions, into two clusters, we can make a distinction between most of the solutions with a penalty which are disqualified and those without.

Figure 2. Parallel Coordinate Plot and Objective Space after K-means clustering the pareto front solutions.

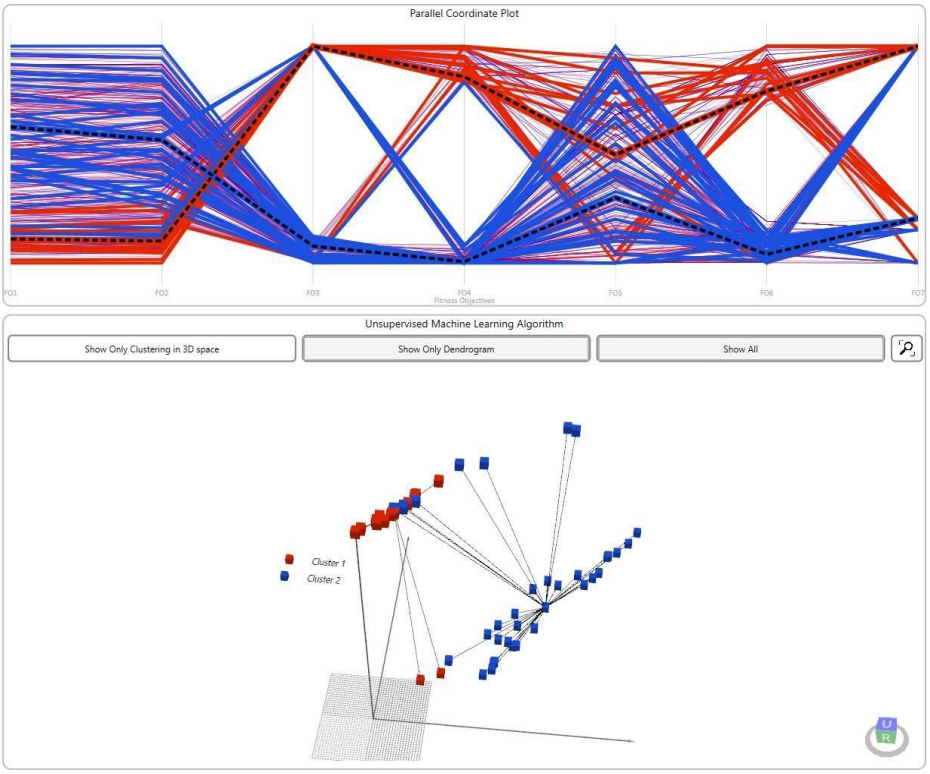

As can be observed in Figure 2, the clustering gives an imperfect yet useful division between the design solutions: the black striped line in Cluster 2, or the blue solutions shows that these trend to solutions that perform rather well compared to the black striped line in Cluster two, or the red solutions. The trade-off appears that Cluster 1 contains mostly facades with much smaller thickness and area, but peak more often in the Parallel Coordinate Plot, showing that they do not perform well because of the penalties which already should disqualify the solutions entirely. Thus the design solutions in Cluster 2 (35 meshes) are exported for further investigation as can be seen in the following Figure 3.

Figure 3. Exported cross-section Phenotypes of Cluster 2.

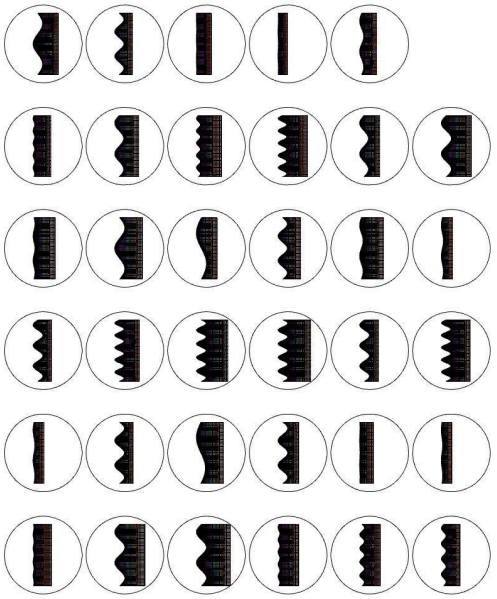

Figure 4. Invalid cross-sections circled in red (R-value < 4.5 W/($m^2 \cdot K$)) and purple (displacement > 1.2 cm).

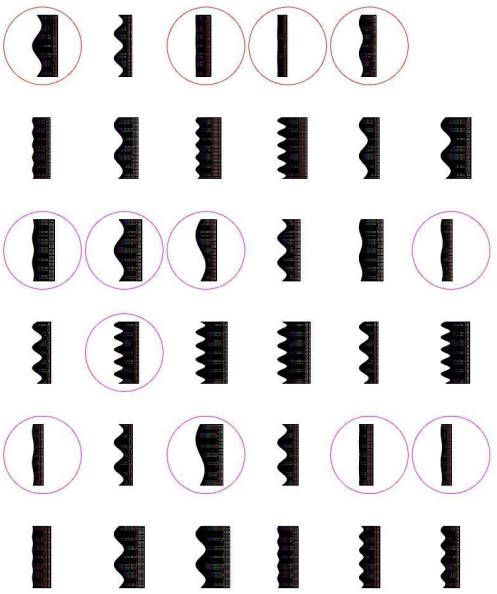

Further observation shows that some of these solutions are disqualified. In Figure 4 the solutions in which the R-value is lower than 4.5 W/($m^2 \cdot K$) and the displacement is larger than 1.2 cm are displayed in red and purple circles respectively. Out of the valid optimal performing solutions we take a closer look at three solutions as seen in the blue circles in Figure 5. These solutions are chosen because they come closest to the desired R-value of 4.5 W/($m^2 \cdot K$). Since the solutions with a very high R-value are valid results of the optimisation process, but overkill for the Dutch regulations, they are discarded. The cross-sections are displayed in more detail along their specifications in Figure 6 and visualised in 3D in Figure 7.

Figure 5. Optimal R-value cross-sections circled in blue.

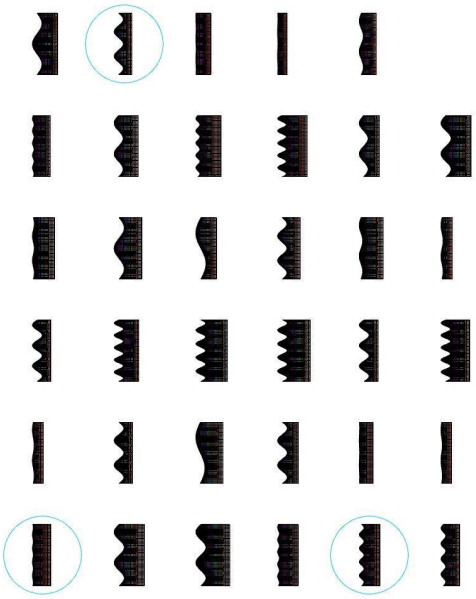

Figure 6. Optimal R-value cross-sections exported as THERM meshes, with temperature in ℃.

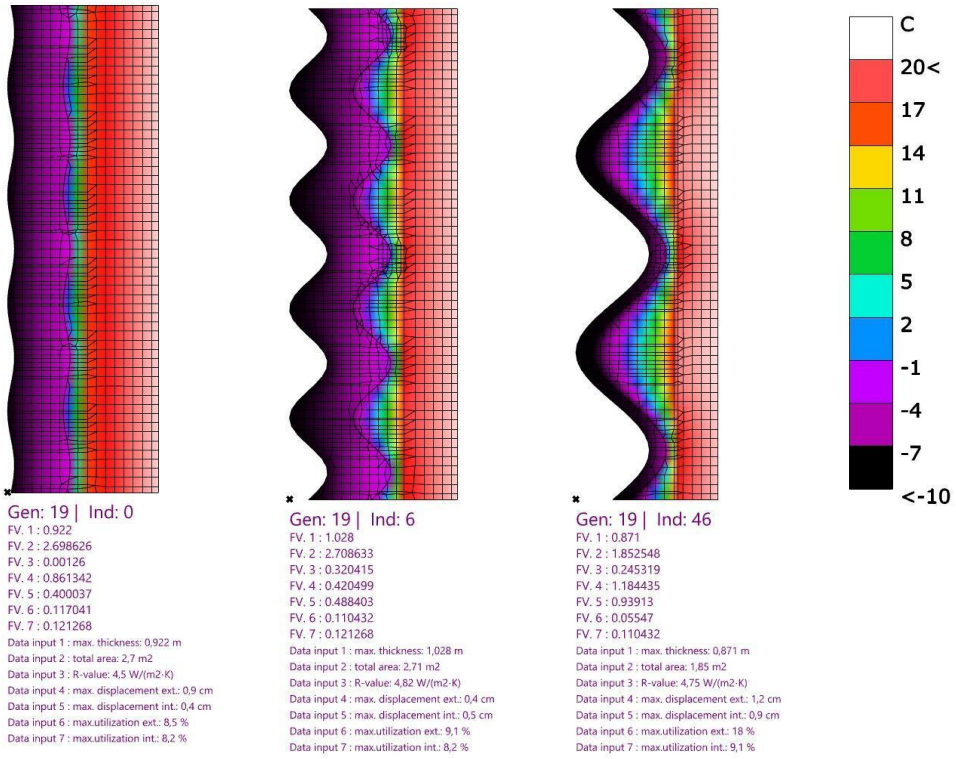

Figure 7. Optimal R-value Phenotypes visualised in 3D.

V. Conclusions

Our overall research question was how the optimisation of an additive manufactured earthen facade for insulating capability and structural integrity is reflected in its architectural morphology. This will be answered by reflecting on the three optimised solutions as found in the previous section.

The conductive and structural properties of the AM earthen mixture are reflected in the final ‘optimal’ morphologies of the facades through a reduction in individual wall thickness, or efficiency, to a level that complies with the minimum wind-load and gravity load on both walls of the cavity wall facade element, because of the poor thermal properties of the material. A thicker wall would be unnecessary when the utilisation or displacement are already below 100% and 1.2 cm respectively. However what is surprising is that while the displacement is getting close to its maximum value in all three ‘optimal solutions’, the utilisation is far below the maximum of 100%. This could be ascribed to the material’s structural properties and the calculated maximum displacement not being in line with its ability to not yet yield under tension when the material begins to deform. As a result of these structural properties of earth the facade elements are of considerable thickness, even when optimised.

By introducing a sinusoidal wave in the exterior wall, a facade morphology is created that would be hard to reproduce without a 3D printer, unlocking new architectural potential, evidencing the influence of the designer on the optimisation process. In the three ‘optimal solutions’ it can be seen that the bigger the amplitude, the thinner the exterior wall gets. Furthermore the three solutions show that a big amplitude in the sinusoidal wave can actually reduce the amount of area used by the wall. The amplitude of the wave positively impacts wall thickness by reducing it, while still achieving valid scores for both utilisation and displacement.

The architectural morphology of an earthen facade has a lot of promise thanks to the form freedom introduced by the 3D printer. At the same time a ‘form follows function’ design theory is enforced through the multi-objective optimisation process. It is up to the designer to implement features in the parametric script that are consistent with their design concept, in order to limit the range of optimised design solutions generated by the multi-objective optimisation. Thus by purely judging the three found facade elements on architectural appeal, it will remain a subjective value judgement. When a flatter wall is preferred, the wall will be thicker and use more earth materials compared to when a sinusoidal wall is chosen. In return less insulation is needed because of the mass of the earth material. By meeting in the middle, another design solution on the Pareto curve might be selected that thus is more efficient in material usage, space usage but might score less on the embodied energy usage through the amount of extra sheep wool insulation. It is up to the designer to find a balance between the architectural appeal and numerical objectives, both when creating the script and during the evaluation of the generated solutions, always keeping in mind the consequences of the following decisions.

VI. Discussion

In the paper there were assumptions made on the material properties of the earthen mixture. Field work should provide more data on whether they were correct. More research is needed on, for example, the impact of drying or stabilisation over time to determine a more accurate Young's Modulus value. Similarly, more research is needed on usable fibres and stabilisers to improve the structural properties of earth mixtures, which would result in different recipes that allow for the construction of more slender walls. Field experiments using different types of insulation would show how applicable sheep wool is as cavity insulation in an earthen facade compared to other insulation materials, considering effects such as condensation and sagging of the material over time.

There are many factors that were not considered when designing the parametric model for the facade, especially in the area of facade requirements. For example, but not limited to, the influence of weather on the erosion of earth, the use of water-proof coatings, the potential risks of condensation occurring in the facade which can be analysed using heat flux evaluation, the need to add openings and how to detail openings such as windows and doors in 3D printed structures. Another factor not considered in this paper is the shrinking of the material after printing. All in all there are potentially many more factors that can be numerically described as Fitness Objectives and could be tested in further studies.

On the subject of the multi-optimisation process: since the blue graphs Figure 1 appear to be relatively stable and not moving much after 20 generations, 1000 solutions appear to be adequate to gain an insight into the specifications and morphology of the generated facades. However it can be seen in the three 'optimal solutions' that even better performing solutions should have been found, since the R-value hasn't fully converged to 4.5 $W/(m^2 \cdot K)$ in all solutions. Remarkable too is that the interior wall width diverged a lot between solutions and has not reached 1.2 cm displacement, even though the relationship between that wall and width, area, utilisation and displacement should be direct. Although a notable exception here is R-value, which might explain the variation in wall thickness by demonstrating that width and area is judged harsher than R-value in the script. Altogether this shows that reducing the range of the parameters and expanding the time spent on optimisation most likely would produce better solutions, but could also indicate that the objectives need refinement.

This research focussed on the material properties of AME and its relationship with thermal and structural performance and did not consider the actual printing process. Research into printed earth as an orthotropic material is needed because of the influence of print directions of the extrusion. Furthermore there is a lack of data on how realistic the modelled facade elements are when taking into account factors such as stabilisation, shrinkage and print speed. 3D print specific follow-up research could also look into using infill patterns to improve material efficiency in the walls even further. Since the morphology of the facade is 2.5D, because of the extrusion from its section, more complicated 3D facades which have different horizontal sections should also be considered for optimisation. The multi-objective optimisation process described in this paper should be seen as a starting point for developing more complex, realistic and better performing AME facade elements.

References

1. Marsh, A. T. M. & Kulshreshtha, Y. (2021). The state of earthen housing worldwide: how development affects attitudes and adoption. *Building Research & Information, 50*(5). pp.485-501. https://doi.org/10.1080/09613218.2021.1953369
2. Hall, M. R., Lindsay, R., & Krayenhoff, M. (2012). 1 – Overview of modern earth building. In M. R. Hall, R. Lindsay, & M. Krayenhoff (Eds.), *Modern earth buildings*, pp.3–16. Woodhead Publishing. https://doi.org/10.1533/9780857096166.1.3
3. Cabeza, L. F., Barreneche, C., Miró, L., Morera, J., Bartolí, E., & Fernández, A. (2013). *Low carbon and low embodied energy materials in buildings: A review. Renewable and Sustainable Energy Reviews, 23*, pp.536–542. https://doi.org/10.1016/j.rser.2013.03.017
4. United Nations, Department of Economic and Social Affairs, Population Division. (2019). *World Urbanization Prospects: The 2018 Revision (ST/ESA/SER.A/420)*. New York: United Nations.
5. Groenemeijer, L., & Van der Lelij, M. (2021). *Inventarisatie plancapaciteit oktober 21*. https://abfresearch.nl/publicaties/inventarisatie-plancapaciteit-mei-2021/
6. Endres, E., Mehnert, J., Hildebrand, L., Schweiker, M., Roswag-Klinge, E., & Knaack, U. (2021). State of the Art and Potentials of Additive Manufactured Earth (AME). In T. Auer, U. Knaack, & J. Schneider (Eds.), *Proceedings of the 9th PowerSKIN Conference* (pp. 203-212). TU Delft Open.
7. A. Perrot, D. Rangeard, & E. Courteille. (2018). 3D printing of earth-based materials: Processing aspects. *Construction and Building Materials, 172,* p.p.670-676, ISSN 0950-0618, https://doi.org/10.1016/j.conbuildmat.2018.04.017
8. Gomaa, M., Vaculik, J., Soebarto, V., Griffith, M., & Jabi, W. (2021). Feasibility of 3dp cob walls under compression loads in low-rise construction. *Construction and Building Materials, 301*, p.124 079. https://doi.org/10.1016/j.conbuildmat.2021.124079
9. Ferretti, E., Moretti, M., Chiusoli, A., Naldoni, L., De Fabritiis, F., & Visonà, M. (2022a). Mechanical Properties of a 3D-Printed Wall Segment Made with an Earthen Mixture. *Materials, 15,* p.438. https://doi.org/10.3390/ma15020438
10. Ferretti, E., Moretti, M., Chiusoli, A., Naldoni, L., & De Fabritiis F., & Visonà, M. (2022b). Rice-Husk Shredding as a Means of Increasing the Long-Term Mechanical Properties of Earthen Mixtures for 3D Printing. *Materials. 15*(3):743. https://doi.org/10.3390/ma15030743
11. Bui, T. T., Bui, Q. B., Limam, A., & Maximilien, S. (2014). Failure of rammed earth walls: From observations to quantifications. *Construction and Building Materials, 51*, p.p.295-302. https://doi.org/10.1016/j.conbuildmat.2013.10.053
12. Ávila, F., Puertas, E., & Gallego, R. (2021). Characterization of the mechanical and physical properties of unstabilized rammed earth: A review. *Construction and Building Materials, 270,* p.121435. https://doi.org/10.1016/j.conbuildmat.2020.121435
13. Araki, H., Koseki, J., & Sato, T. (2016). Tensile strength of compacted rammed earth materials. *Soils and Foundations, 56*(2)*,* p.p.189-204. https://doi.org/10.1016/j.sandf.2016.02.003
14. Feng, S. (2022). The structural design of earthen structures with robotic shotearth fabrication. [Master's Thesis, Delft University of Technology]. Repository TU Delft. http://resolver.tudelft.nl/uuid:043f06c6-e440-4387-93fb-fc3fd8b69bf9
15. Farouki, O. T. (1981) The thermal properties of soils in cold regions. *Cold Regions Science and Technology, 5*(1), p.p.67-75. https://doi.org/10.1016/0165-232X(81)90041-0
16. Rubio, E. Caselles, V.Badenas,C. (1997). Emissivity measurements of several soils and vegetation types in the 8–14, µm Wave band: Analysis of two field methods. *Remote Sensing of Environment, 59*(3), p.p.490-521. https://doi.org/10.1016/S0034-4257(96)00123-X
17. Arends, J., Snijder, A., Van Vliet, B., & Brancart, S. (2022). *Vademecum voor draagconstructies van gebouwen*. Chair of Structural Design and Mechanics, Delft.
18. Asdrubali, F., D'Alessandro, F., & Schiavoni, S. (2015) A review of unconventional sustainable building insulation materials. *Sustainable Materials and Technologies, 4*, p.p.1-17. ISSN 2214-9937. https://doi.org/10.1016/j.susmat.2015.05.002

VII. Appendix

Appendix Table 1. THERM and Karamba3D inputs.

THERM property	**Value**	**Unit**
Exterior boundary condition	-10	℃
Interior boundary condition	20	℃
Karamba3D property	**Value**	**Unit**
Exterior load local to mesh	0.7	kN/m^2
Interior load local to mesh	0.3	kN/m^2
Material Type	Isotropic	n.a.

Appendix Figure 1. Grasshopper script:

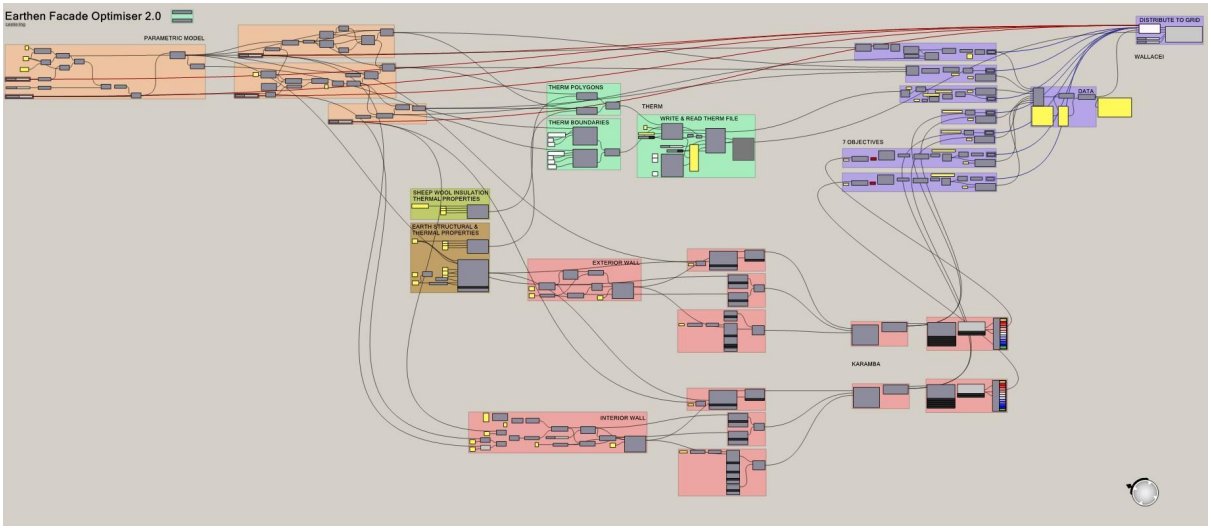

Appendix Figure 2. Karamba3D Model View and Shell View.

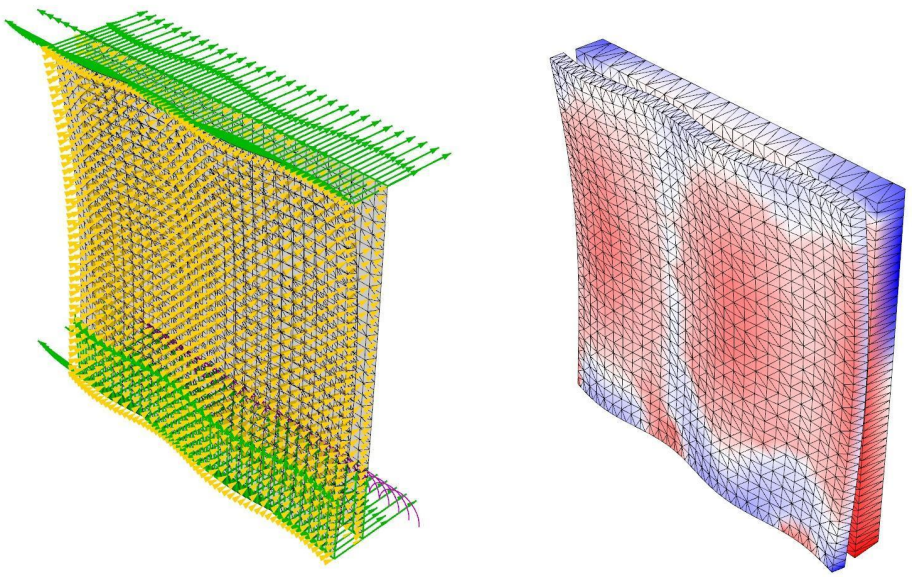

Appendix Figure 3. Wallacei settings.

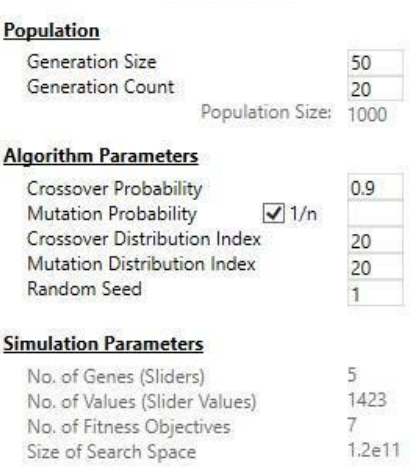

Appendix Figure 4. Wallacei RunTime.

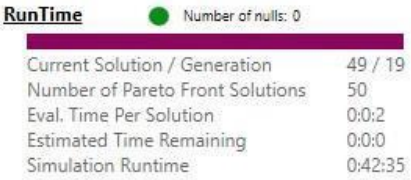

Appendix Figure 5. K-means clustering settings.